

Lennard-Jones potential model for the condensed phases of C_{70}

M. Pickholz and Z. Gamba

Comisión Nacional de Energía Atómica, Departamento de Física, Avenue Libertador 8250, (1429) Buenos Aires, Argentina

(Received 2 August 1995)

A simplified site-site Lennard-Jones (LJ) model for the intermolecular potential of C_{70} is studied by a series of classical constant-pressure molecular-dynamics calculations of C_{70} crystals, at several temperatures and zero pressure. The molecular model approximately simulates the real molecular volume and form and consists of 12 LJ interaction sites arranged in a polyhedra of D_{5h} symmetry. It is found that this simple model reproduces many properties of cubic and hexagonal crystals of C_{70} , although further improvement is needed, mainly in the temperatures of the successive phase transitions.

I. INTRODUCTION

At room temperature C_{70} crystallizes in two possible phases: cubic fcc ($\sim 90\%$ of the samples) and hexagonal. The last one is metastable: in several days the hexagonal crystals show an irreversible structural transformation to the fcc phase.^{1,2} Above 360 K both crystals are in a plastic phase: the centers of mass show a regular array and the molecules reorientate continuously to achieve, in a temporal average, the corresponding crystal site symmetry.^{1,3} Upon cooling, these crystals exhibit two first-order phase transitions, due to a sequential orientational ordering of the C_5 molecular axis first, and then about that axis.

The hexagonal crystals show, on cooling, a first-order phase transition from a hcp phase ($c/a=1.63$) to a hexagonal lattice ($c/a\approx 1.82$), with all molecules aligned along the crystallographic c axis and reorientating continuously around it.¹ At lower temperatures there is a transition to an orientationally ordered monoclinic structure with doubling of the unit cell ($Z=4$). In hexagonal coordinates the monoclinic $P112_1/m$ unit-cell parameters are: $a_m=b_h$, $b_m=c_h$, $c_m=2a_h$, $\beta=120^\circ$. Afterwards it was pointed out that this structure corresponds to an orthorhombic $Pnma$.⁴

The fcc crystals instead transform, on cooling, in rhombohedral crystals with all molecules aligned along $[111]$ and with a uniaxial rotation around the long molecular axis.⁵⁻⁷ Single crystals cannot be preserved through this first-order phase transition, although the cubic phase can be easily supercooled.^{8,1,2} The low-temperature structure is monoclinic, a slight distortion of the rhombohedral structure.² This structure has not been determined.

These phase transitions show a large thermal hysteresis and the transition temperatures (T_c) are strongly dependent on the purity and thermal evolution of the sample.^{9,1} A modulated differential scanning calorimetry,⁹ for example, has located them at 360 and 280 K in cubic crystals and 350 and 300 K in hexagonal crystals. Other measurements show deviations of about 10–30 K from these values.^{1,6,8,10}

Numerical simulations at 100, 300, and 500 K, using a rigid molecular model with a nonbonded Lennard-Jones (LJ) model between the 70 C atoms, show good agreement with experimental data, although the configurational energy is calculated too high.¹¹ At 100 K, this model calculates a pseudohexagonal structure ($ABAB$ array) to be slightly more

stable than the pseudocubic one ($ABCABC$ array). Sprick *et al.*¹² improved the model by adding a set of distributed charges on C atoms and short bonds. A series of molecular-dynamics (MD) simulations on cubic C_{70} crystals predicted a fcc to trigonal phase transition at ≈ 380 K and a trigonal to monoclinic transition at ≈ 200 K. No calculations on hexagonal crystals are reported.

Despite the excellent results, this type of detailed semiempirical model shows two problems. The first one is that the charge distribution for C_{70} is based on estimations for C_{60} ,¹³⁻¹⁵ but a subsequent molecular-orbital calculation¹⁶ determined that the real charge distribution within C_{60} might be several times lower than those estimated. This fact suggests, by similarity with other molecular crystals in which the electrostatic interactions are negligible, that the molecular volume and polarizability are the main factors to determine the intermolecular interactions and that they, in turn, might be approximately reproduced by a semiempirical atom-atom model.¹⁷ The second problem is that the large amount of interaction centers makes prohibitive a study of the static and dynamical properties of large samples of molecules in pure or doped phases, in bulk or in two-dimensional problems, and for different thermodynamic states.

In a recent paper we proposed, as a first approach to the real potential, a simple site-site LJ intermolecular potential model for the condensed phases of C_{70} .¹⁸ The model consists of 12 LJ interaction sites, arranged in a polyhedra of D_{5h} symmetry. The reduction in the number of interaction sites makes affordable the above-mentioned studies. The model can also be of theoretical interest, since it allows to study the phase diagram of molecules with D_{5h} symmetry. In particular, of the solid phases introduced by the broken I_h symmetry of the parent molecule C_{60} . Lattice sums calculations over suggested low-temperature structures for C_{70} imply that, at 0 K, those with fcc or hexagonal packing show the lowest configurational energy.¹⁸ Here we study the orientationally ordered and disordered phases of C_{70} , as given by this model, by performing a series of classical constant-pressure molecular-dynamics (MD) simulations at several temperatures and zero pressure, in the (NPH) ensemble. This method allows fluctuations of the volume and shape of the MD box and is therefore useful to search the stable crystal-line configuration at each point of the phase diagram.

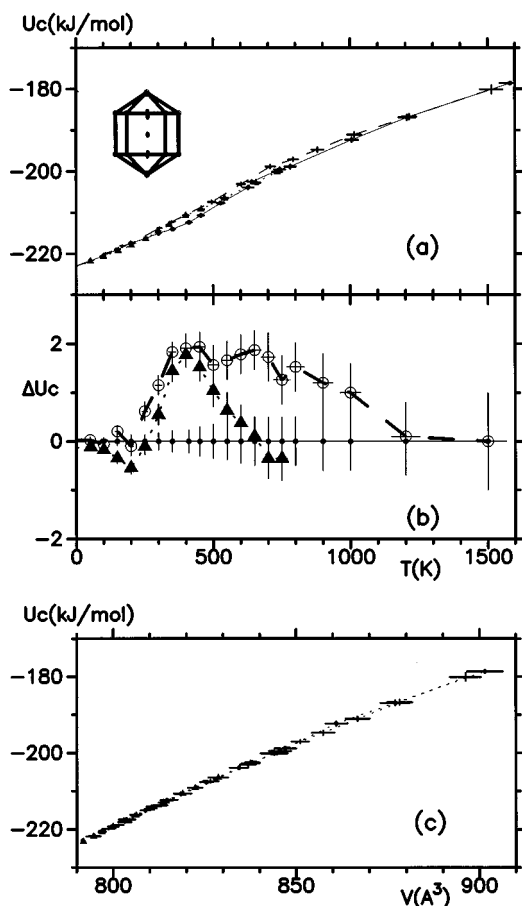


FIG. 1. (a) Evolution on heating of the configurational energy U_{conf} of cubic (solid line), trigonal (solid triangles), and hexagonal crystals (dashed line). (b) Difference ($U_{\text{conf}}^h - U_{\text{conf}}^c$) (empty circles) and ($U_{\text{conf}}^t - U_{\text{conf}}^c$) (solid triangles). (c) Relationship between U_{conf} and V for all samples.

II. THE INTERMOLECULAR POTENTIAL MODEL

This simplified LJ intermolecular potential model was developed for the crystalline phases of C_{60} (Ref. 19) and afterwards transferred to C_{70} crystals.¹⁸ The molecular volume and form of these molecules can be approximately reproduced by a 12 LJ sites polyhedra of, respectively, I_h or D_{5h} symmetry. The 12 LJ interaction sites are located in the direction of the 12 pentagonal faces, conserving then the molecular symmetry. For C_{70} , the anisotropy of the polyhedra with D_{5h} symmetry is set equal to that of the real molecule (inset in Fig. 1).¹⁸

The 12 sites are located inside the real molecules.^{18,19} This reduction was found necessary to reproduce the Q_0 and $Q_{6,0}$ electrostatic molecular multipolar moments of C_{60} , the first ones different from zero when the molecule is charged (C_{60}^- in doped crystals). With this reduction it is also possible to simulate, with few interaction sites and a relatively large LJ parameter σ , the molecular volume and potential contour. In our simulations the inertial molecular moment is rescaled to its real value, to avoid modifications in the equations of motion. The coordinates and LJ parameters ($\epsilon = 1.0208$ kJ/mol, $\sigma = 6.20$ \AA) of the 12 sites for C_{70} were given in Ref. 18.

III. CALCULATIONS

Using the proposed model, we perform a series of classical constant-pressure MD simulations^{20,21} of C_{70} crystals, in the (NPH) ensemble. The molecules are considered as rigid bodies and the motion of their centers of mass is followed with a third-order predictor-corrector algorithm, their orientations with quaternions and a fourth-order algorithm. The time step is of 0.0035 ps and the cutoff radius for the intermolecular interactions is of 16 \AA . Nevertheless, correction terms due to the truncated tail of the potential are taken into account.

The crystals were studied at several temperatures in the range of 50–1500 K and zero pressure. Although there is some controversy about the fusion temperature (T_f) of fullerenes,^{22,5} the point at $T = 1500$ K was included after an estimation of $T_f \approx 1800$ K for C_{60} crystals,^{23,24} and considering that it should be higher for C_{70} crystals.

The samples consisted of 256 C_{70} molecules initially located in a fcc ($ABCABC$) or in an hexagonal ($ABAB$) array. Three series of MD runs, referred to as “cubic,” “trigonal,” and “hexagonal,” were performed. The corresponding initial configurations, at low temperatures, are an ordered $Pa3$ structure (cubic sample), a fcc array with all molecules aligned along one main diagonal (trigonal sample) and an orthorhombic $Pnma$ structure for the pseudohexagonal crystals (hexagonal sample).⁴ Sample size effects have been tested with a MD box of 108 molecules, obtaining similar results. At each point of the phase diagram the MD samples are equilibrated for 5000 to 10 000 time steps. The crystals were studied first upon heating and their thermal hysteresis by a subsequent cooling.

IV. RESULTS

The three series show quite similar values of configurational energy U_{conf} as a function of temperature T [Fig. 1(a)]. At high temperatures this is an expected behavior: in the plastic phases the molecules are very nearly spherical, and this is a known result for LJ systems, in which the difference in energy between fcc and hcp arrays is less than 0.001%.²⁵ At 50 K we calculate $U_{\text{conf}} = -221.7$ kJ/mol, equal for ordered cubic (U_{conf}^c) and hexagonal (U_{conf}^h) crystals. Figure 1(b) shows that the difference $\Delta U^{hc} = (U_{\text{conf}}^h - U_{\text{conf}}^c)$ is zero up to 200 K and then increases to a maximum of ~ 2 kJ/mol at ~ 400 K. At low temperatures, our cubic $Pa3$ sample does not transform spontaneously to the rhombohedral phase and this was the reason to include a trigonal series in our study. At 50 K this sample is slightly more stable than the cubic one, $U_{\text{conf}}^t = -221.8$ kJ/mol. The difference increases with T , at 200 K is $\Delta U^{tc} = (U_{\text{conf}}^t - U_{\text{conf}}^c) \approx -0.5$ kJ/mol. For still higher temperatures, ΔU^{tc} changes sign and is $U_{\text{conf}}^t \sim U_{\text{conf}}^h$, both higher than U_{conf}^c . The trigonal sample approaches again the cubic one once the C_5 axis of the molecules are orientationally disordered. Figure 1(c) shows that the relationship between U_{conf} and the volume per molecule (V) is the same for the three series.

The heat of sublimation has been measured at 739 K, $\Delta H_{\text{sub}} = 180(9)$ kJ/mol.²⁶ Using our interpolated value of $U_{\text{conf}} \approx 199$ kJ/mol, it can be estimated $\Delta H_{\text{sub}} \approx -2RT$

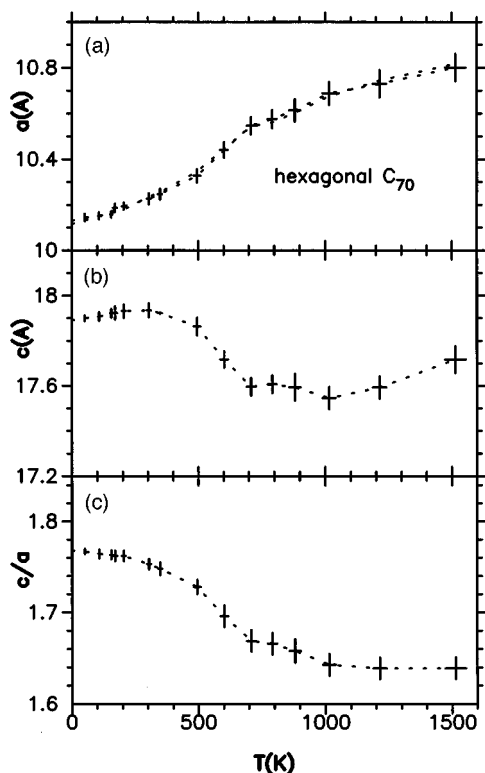


FIG. 2. Evolution on heating of the unit-cell parameters for hexagonal crystals: (a) a and b axes, (b) c axis, (c) c/a relationship.

$-U_{\text{conf}} = 187$ kJ/mol, in good agreement with the experimental data.

All reported quantities and plots have been measured on heating. A subsequent cooling reveals that there is considerable hysteresis, due to a certain amount of statical orientational disorder that persist at low temperatures. This disorder introduces larger differences in configurational energy (~ 2 – 4 kJ/mol at 50 K) than that between cubic and hexagonal phases and that between samples of 108 and 256 molecules (~ 0.3 kJ/mol at 50 K).

Cubic and trigonal samples conserved the $ABCABC$ array of the molecular centers of mass at all temperatures. None of the crystals show diffusion, the centers of mass librate with an amplitude of ≈ 0.07 Å at ≈ 100 K, and of 1.3 Å at 1500 K. At room temperature the calculated fcc lattice parameter is $a = 14.80$ Å upon heating and $a = 14.83$ Å upon cooling, in reasonable accord with a measured value $a = 14.90$ Å.^{6,8} The fcc unit-cell angles remain at $\alpha = \beta = \gamma = 90^\circ$, with a deviation of 0.4° at 50 K and 0.8° at 1500 K. The trigonal cell angles are $\sim 86.9^\circ$ at 50 K, tending to 90° with increasing temperature, in the plastic phase. At 300 K the fcc lattice distortion is measured to be $\alpha \approx 88$ – 89° ,^{1,5} our calculated values are $a = 14.82(4)$ Å and $\alpha = 87.2(2)^\circ$.

The hexagonal crystals conserved also the $ABAB$ array at all temperatures, but show a strong variation in their unit-cell parameters [Figs. 2(a), 2(b), and 2(c)]. The unit-cell angles remain at $\alpha = \gamma = 90^\circ$, $\beta = 120^\circ$, their fluctuation is at most of $\approx 0.7^\circ$ at 1500 K. At low temperatures and up to 300 K a normal thermal expansion can be observed, the molecules are aligned along the crystallographic c axis and in this range of temperatures they start to spin about the long molecular axis. This was determined by studying the molecular orien-

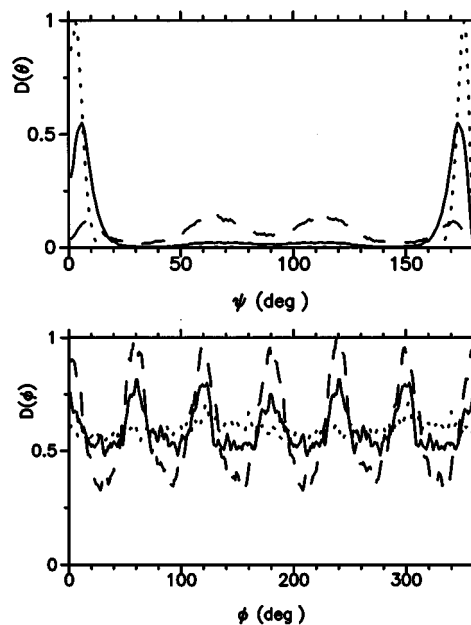


FIG. 3. Orientational probability $D(\theta)$, $D(\phi)$ in polar angles, of the large molecular axis in hexagonal crystals. θ is measured from crystallographic c axis. $T = 150$ K (dotted line), 400 K (full line) and 900 K (dashed line).

tations as a function of time and measuring reorientational times and orientational probabilities. At 200 K the calculated hexagonal lattice parameters are $a = 10.2$ Å, $c = 17.95$ Å, $c/a = 1.76$, which can be compared with the experimental values $a = 10.02$ Å, $c = 18.53$ Å, $c/a = 1.85$.² At higher temperatures the C_5 molecular axis starts its reorientation, which in turn implies an expansion in a and b axes and the molecular array tends to a close packing with $c/a = 1.63$ [Fig. 2(c)]. Once the molecules are orientationally disordered, the lattice shows again the normal variation due to thermal expansion.

At low temperatures our pseudohexagonal structure belongs to the orthorhombic $Pnma$ group. It is similar to that suggested in Refs. 1, 2, and 4, except that the molecules are rotated 12° in their equatorial plane (similar to the structure in Ref. 18).

The orientational probabilities of the molecular C_5 axis were studied, for all samples, in polar angles θ , ϕ , where θ is measured from the c crystallographic axis. At low temperatures, all molecules of cubic crystals have their C_5 axis along a main diagonal ($\theta = \pm 54.7^\circ$, $\phi = 45, 135, 225, 315^\circ$), characteristic of the $Pa3$ structure. The amplitude of libration and orientational disorder of the long axes increases with temperature, but even in the plastic phase the motion is slightly hindered and the profile exhibits the crystalline local site symmetry. The behavior is similar in the trigonal sample, except that at low temperatures all molecules are parallel to the main diagonal. Figure 3 shows the orientational probabilities $D(\theta)$, $D(\phi)$ in hexagonal crystals. At low temperatures, $T \lesssim 300$ K all molecules are aligned along the c axis ($\theta = 0, 180^\circ$). Up to ≈ 400 K the molecules show a small tilt angle ($< 10^\circ$) and at higher temperatures, in the plastic phase, there is a preferred orientation angle of $\theta \approx 65^\circ$. This distribution can be interpreted as a precessional motion, similar to that observed in the hexagonal phase of N_2 , where

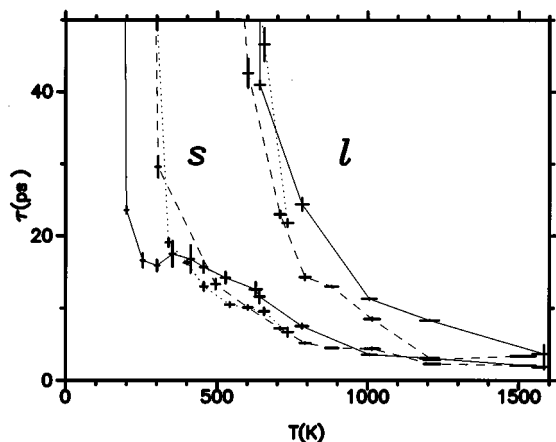


FIG. 4. Reorientational times τ_2 for large (l) and short (s) molecular inertial axes in cubic (full lines), trigonal (dotted lines), and hexagonal (dashed lines) crystals. The lines are a guide to the eyes.

the molecules have a precession angle of $\theta \approx 55^\circ$.²⁷ In our case the motion of the C_5 axis is dynamically disordered between symmetrically equivalent orientations, with larger times spent librating in these orientations.

The characteristic reorientational time τ_2 is obtained from the second-order self-correlation functions for the orientation of long and short inertial axes. Figure 4 shows $\tau_2(T)$ for the different samples. The successive reorientational phase transitions can be located from this data, assuming a transition when a reorientational time goes to infinite. At $T=1500$ K cubic and hexagonal crystals show a characteristic time of a few ps. Below ~ 600 K a slowing down can be observed in the reorientation of the long axes and an increasing number of molecules that keep it fixed. Below ~ 300 K, a similar behavior is observed for the spinning motion about the long

axis. Our calculations shows accord with a NMR measurement of about 15 ps at 340 K.³

The vibrational density of states is calculated as the Fourier transform of the velocity self-correlation functions. Comparison with neutron²⁸ and Raman²⁹ data shows that our band of lattice frequencies, that spans up to 40 cm^{-1} , is calculated $\approx 30\%$ low. The contribution of the reorientational motion exhibit two broad peaks that, in correspondence with the evolution of the reorientational times τ_2 , tend to zero frequencies with increasing temperature.

V. CONCLUSIONS

In this paper we study a simplified atom-atom model of the intermolecular potential of C_{70} crystals, that consists of 12 LJ sites in a D_{5h} array. The LJ parameters are transferred from a previous study on C_{60} crystals.

A series of classical constant-pressure MD simulations of cubic and hexagonal crystals shows that this simple model reproduces many features of the phase diagram of C_{70} crystals. In general, the calculated lattice parameters and configurational energies are very close to the experimental values. Also the thermal hysteresis and the sequence of successive reorientational phase transitions is obtained.

Nevertheless the model needs further improvements: the temperature corresponding to the reorientation of the long molecular axis is calculated too high, which implies a need to reduce the difference between long and short axes. On the other hand, the lattice frequencies and c/a relationship of pseudohexagonal crystals are low, which might imply a need for larger angular variations of the potential in the equatorial plane. An accurate measurement of the ordered low-temperature structure and lattice frequencies can allow a further refinement of the model. Nevertheless, in its present form this simple model is useful to obtain a qualitative picture of the complex phase diagram of C_{70} crystals.

¹G. van Tendeloo *et al.*, *Europhys. Lett.* **21**, 29 (1993).

²M. A. Verheijen *et al.*, *Chem. Phys.* **166**, 287 (1992).

³R. Tycko *et al.*, *J. Chem. Phys.* **99**, 7554 (1993), and references therein.

⁴W. Que *et al.*, *Phys. Rev. B* **47**, 13 074 (1993).

⁵H. Kawamura *et al.*, *J. Phys. Chem. Solids* **54**, 1675 (1993).

⁶C. Cristides *et al.*, *Europhys. Lett.* **22**, 611 (1993).

⁷K. Misof *et al.*, *Europhys. Lett.* **22**, 585 (1993).

⁸C. Meingast *et al.*, *Appl. Phys. A* **56**, 227 (1993).

⁹A. R. McGhie *et al.*, *Phys. Rev. B* **49**, 12 614 (1994).

¹⁰E. Grivei *et al.*, *Phys. Rev. B* **47**, 1705 (1993).

¹¹A. Cheng and M. L. Klein, *Phys. Rev. B* **46**, 4958 (1992).

¹²M. Sprik *et al.*, *Phys. Rev. Lett.* **69**, 1660 (1992).

¹³X. P. Li *et al.*, *Phys. Rev. B* **46**, 4301 (1992).

¹⁴M. Sprik *et al.*, *J. Phys. Chem.* **96**, 2027 (1992).

¹⁵E. Burgos, *Phys. Rev. B* **47**, 13 903 (1993).

¹⁶T. Yildirim *et al.*, *Phys. Rev. B* **48**, 1888 (1993).

¹⁷A. I. Kitaigorodski, *Molecular Crystals and Molecules* (Academic, New York, 1973).

¹⁸M. Pickholz and Z. Gamba, *J. Chem. Phys.* **100**, 4531 (1994); *ibid.* (to be published).

¹⁹Z. Gamba, *J. Chem. Phys.* **97**, 553 (1992).

²⁰S. Nose and M. L. Klein, *Mol. Phys.* **50**, 1055 (1983).

²¹R. W. Impey *et al.*, *Mol. Phys.* **50**, 243 (1983).

²²N. W. Ashcroft, *Nature (London)* **365**, 387 (1993).

²³A. Cheng *et al.*, *Phys. Rev. Lett.* **71**, 1200 (1993).

²⁴M. H. J. Hagen *et al.*, *Nature (London)* **365**, 425 (1993).

²⁵Y. Choi *et al.*, *J. Chem. Phys.* **99**, 9917 (1993).

²⁶C. Pan *et al.*, *J. Phys. Chem.* **95**, 2944 (1991).

²⁷A. F. Schuch and R. L. Mills, *J. Chem. Phys.* **52**, 6000 (1970).

²⁸B. Renker *et al.*, *Z. Phys. B* **90**, 325 (1993).

²⁹P. H. M. van Loosdrecht *et al.*, *Phys. Rev. B* **47**, 7610 (1993).